J. Fluid Mech. (1990), *vol.* 211, *pp.* 183–209
Printed in Great Britain

Oscillating flows over periodic ripples

By TETSU HARA AND CHIANG C. MEI
Ralph M. Parsons Laboratory, Department of Civil Engineering, Massachusetts Institute of Technology, Cambridge, MA 02139, USA

(Received 9 January 1989)

Oscillating flows over periodic ripples are of practical as well as scientific interest because of their relevance to beach processes. When either the ripples are sufficiently steep or the amplitude of ambient oscillations large, streamlines of a viscous flow are no longer parallel to the ripple surface. Circulation cells are formed which can help redistribute suspended sediments. Here we study theoretically these cells for a low-viscosity fluid such as pure water over rigid ripples. In particular we have calculated cells whose dimensions are as large as the ripple wavelength and therefore represent viscous effects far above the usual Stokes boundary layer. An idea of Stuart which was originated for stationary mean circulations around a cylinder is extended here. For large ambient amplitude, large oscillating vortices drifting with the ambient flow are found by seeking the stationary cells in a moving coordinate system.

1. Introduction

Sand ripples are frequently found on beaches under the influence of surface waves. When the amplitude of the water oscillation is sufficiently large, vortices are formed in the lee of every crest. Since much dissipation takes place in these vortices, the rate of damping of the surface waves must increase. Vortices are also effective in dislodging sand particles and keep them in suspension, hence they contribute to the evolution of the ripples themselves as well as the transport of sediments by waves and currents. The flow above natural ripples is often turbulent and coupled to the motion of sand, hence theoretical analysis is extremely difficult. Past analyses in the literature of coastal engineering have been empirical and concerned with the effect on the friction factor; the detailed mechanism is usually bypassed. When the amplitude of the ambient oscillations is very weak, however, laminar flows can occur; this situation is easy to realize in the laboratory, especially with rigid and smooth ripples. A theoretical study of laminar oscillatory flows over smooth rigid ripples is of course simpler, and is a helpful first step towards a better understanding of the turbulent, two-phase problem in nature. Not all motivated by beach processes, several authors have undertaken such studies.

Because the typical wavelength of sand ripples is $O(10\text{ cm})$ or less, while that of the gravity waves is $O(10\text{ m} \sim 100\text{ m})$, $K/k \ll 1$ where K and k are respectively the gravity wavenumber and the ripple wavenumber. The local mechanics of ripples within the scale of a few ripple lengths should not be directly affected by the gravity wavelength. If the water depth h is such that $Kh = O(1)$, then the free surface is far above the seabed as far as the ripples are concerned. Here we shall only consider the approximate model in which $kh \to \infty$ and $K/k \to 0$, implying that the gravity waves are infinitely long and the free surface is infinitely far away. The viscous region near the rippled bed then lies beneath a large depth of inviscid fluid. The global effects of

gravity wavelength are manifest over a much longer scale and can be studied by a multiple scale analysis. This will not be pursued here. The important physical parameters in the laminar problem are the frequency ω, the amplitude A of ambient oscillation, the ripple wavenumber k and amplitude a, and the fluid viscosity ν. From these one can define three dimensionless numbers: the ripple slope $\epsilon = ka$, the Keulegan–Carpenter number $\alpha = kA$, and the viscosity parameter $\sigma = k\delta$ where $\delta = (\nu/\omega)^{\frac{1}{2}}$ is the thickness of the Stokes boundary layer.

It is well known that at the outer edge of the Stokes layer, the tangential component of the induced streaming velocity does not always vanish and has a finite limit U_s (see Schlichting 1955). Stuart (1963) was the first to point out, for a cylinder of radius $1/k$, that if the Reynolds number based on the induced streaming $R = U_s/k\nu$ is large, an outer boundary layer of thickness $\delta_s = O(k^{-1}R^{-\frac{1}{2}})$ must exist. In this thicker layer convective inertia and viscous diffusion are equally important. Riley (1967) and Wang (1968) further clarified that if $R \ll 1$ viscous diffusion alone dominates outside the Stokes layer, and therefore the problem may be linearized both inside and outside the Stokes layer. On the other hand, when $R \geqslant O(1)$, the equation governing the steady streaming in the outer layer becomes fully nonlinear. In the ripple problem here the velocity U_s is of $O(\omega kA^2)$ if $A \ll a \sim 1/k$ and $O(\omega kaA)$ if $a \ll A \sim 1/k$ (see later analysis). In the first case, $R = (A/\delta)^2 = (\alpha/\sigma)^2$ while in the second $R = (aA/\delta^2) = \alpha\epsilon/\sigma^2$. For small enough viscosity $\sigma \ll 1$ so that $R \geqslant O(1)$, in both cases an outer layer must exist. The corresponding layer thicknesses are respectively $\delta_s/\delta = O(kA)^{-1} = O(\alpha)^{-1}$ and $\delta_s/\delta = O(\alpha\epsilon)^{-\frac{1}{2}}$.

In existing literature on oscillatory flows over rippled surfaces, only the case of $R \ll 1$ has been treated, in which the Navier–Stokes equations can be linearized. The first theory was given by Lyne (1971) who gave a perturbation analysis for small ϵ/σ to $O(\epsilon/\sigma)$. He calculated the steady streaming and found stationary cells inside the Stokes layer for both small and large α. These cells can keep the sediments in suspension, once the latter are mobilized by the stronger oscillatory flow. Since by definition small ϵ/σ implies small a/δ, the ripples in his theory must be completely immersed in the Stokes layer. Sleath (1974*a*) assumed both small α and small ϵ, and obtained the cellular pattern of Lagrangian mass transport, including the long-scale modulation of the ambient flow due to wave motion. Kaneko & Honji (1979) introduced a perturbation analysis for small α but finite ϵ/σ, and found reasonable agreement with experiments when $\epsilon/\sigma < 0.7$. The experiments were performed in a glycerin/water mixture whose viscosity is 100 times that of pure water; the corresponding σ was $0.1 \sim 0.6$ and not small. The induced streaming recorded photographically is again a feature within the Stokes layer. Matsunaga, Kaneko & Honji (1981) first linearized the Navier–Stokes equations by assuming small α, and solved the initial-value problem numerically to obtain the steady streaming at $O(\alpha)$ under periodic forcing. Their calculation agreed well with the observed flow patterns for $\epsilon = 0.45$ and $\sigma = 0.05 \sim 0.6$. Recently Vittori (1989) has extended Lyne's theory to $O(\epsilon/\sigma)^2$ for $\alpha = O(1)$. She calculated only the steady streaming by solving numerically the first- and second-order Navier–Stokes equations. In her analysis, the Stokes layer thickness is also much greater than the ripple amplitude, which is not the case for most ripples in nature.

For finite ϵ and α, discrete numerical methods have been applied to initial-value problems of the full Navier–Stokes equations by Sleath (1974*b*, 1975), Sato, Mimura & Watanabe (1984), and Shum (1988), for parameters directly relevant to pure water. One of the main results is the presence of oscillating vortices whose dimensions and heights above the ripples are comparable with the ripple wavelength, and much

greater than the Stokes layer thickness. In these works accurate computations are costly; detailed results are not easy to obtain. There are also related analytical and numerical theories for oscillating flows through a furrowed channel by Sobey (1980, 1982, 1983) and Ralph (1986). The objectives and the physics of these studies are rather different because the width of the channel is comparable with the ripple length.

For cases where an outer layer of convective inertia is present, induced streaming has been studied before for cases where the free surface waves are of direct relevance. For the mass transport beneath a standing wave on a horizontal seabed this topic has been examined by Mei, Liu & Carter (1972), Dore (1976), Liu & Davis (1977), all of whom deduced the Blasius boundary-layer equations as did Stuart (1963) for a cylinder. But these theories need revision at the point where two neighbouring boundary layers converge and must turn vertically upwards (see Davidson & Riley 1972 for a circular cylinder). Haddon & Riley (1983) overcame this difficulty by using the full nonlinear steady Navier–Stokes equations, and obtained numerical results valid in the outer layer and in the region of upward flow. For an uneven seabed Riley (1984) has also analysed the mass transport in the outer layer over periodic bars whose wavelength is comparable with the free surface wavelength and the sea depth.

In this paper we shall study two-dimensional laminar oscillations of a fluid with low viscosity, bounded on one side only by a spatially periodic rigid wall. Responses will be assumed to be strictly periodic in time. Two complementary cases will be studied by combining analytical approximations and numerical computations; (i) small α but finite ϵ, and (ii) small ϵ but finite α. In both of them the fluid viscosity is so low that $R \geqslant O(1)$, therefore our parameter regime is different from those in earlier analytical studies and corresponds to situations that can be tested in the laboratory with water.

In Case (i) we first carry out the usual analysis for the Stokes boundary layer, and obtain the steady Eulerian streaming velocity just outside the Stokes layer. The outer layer of convective inertia is then examined. Stationary cells of steady streaming in the outer layer are found; they are of dimensions comparable with the ripple wavelength. Effects of increasing ripple slope is explored.

In Case (ii), the goal is to find oscillating vortices high above the ripples. We accomplish this by first employing a coordinate system oscillating with the ambient fluid. Cells of induced streaming, stationary with respect to the oscillating coordinate system and in the outer layer, are calculated. Upon returning to the stationary frame of reference, these cells are precisely the viscous vortices oscillating to and fro high above the ripples. The amplitude of their displacement is the same as that of the ambient fluid and is therefore comparable with the ripple length; their strength never decays with time. These results are quite consistent with the numerical solution of initial-value problems based on the full Navier–Stokes equations, but shed more light on the mechanism of oscillating vortices over a rippled bed.

2. Formulation in orthogonal coordinates

We shall employ the well-known conformal mapping (Benjamin 1959; Lyne 1971)

$$z' = \zeta' + \mathrm{i}a\mathrm{e}^{\mathrm{i}k\zeta'} \tag{2.1}$$

so that the space above the rippled wall in the $z' = x' + \mathrm{i}y'$ plane maps onto the upper half-plane of $\zeta' = \xi' + \mathrm{i}\eta'$. In real coordinates the mapping is defined by

$$x' = \xi' - a\mathrm{e}^{-k\eta'} \sin k\xi'; \quad y' = \eta' + a\mathrm{e}^{-k\eta'} \cos k\xi'. \tag{2.2a, b}$$

The constant coefficient a is a measure of the ripple amplitude. The Jacobian of transformation is

$$J = \frac{\partial(x', y')}{\partial(\xi', \eta')} = 1 - 2ka\, e^{-k\eta'} \cos k\xi' + (ka)^2 e^{-2k\eta'}. \tag{2.3}$$

We shall assume that $\epsilon \equiv ka$ is always less than 1 at which limit the crests of the ripples become cusps. While a more general transformation can in principle be used by adding higher harmonics, (2.1) is sufficiently versatile for describing all ripples qualitatively.

Let the velocity vector be expressed in both planes by

$$\boldsymbol{u}' = u'\boldsymbol{i} + v'\boldsymbol{j} = U'\boldsymbol{e}_\xi + V'\boldsymbol{e}_\eta, \tag{2.4}$$

where $\boldsymbol{e}_\xi$ and $\boldsymbol{e}_\eta$ are unit vectors along $\eta' =$ constant and $\xi' =$ constant respectively. Since

$$\boldsymbol{e}_\xi = \frac{1}{J^{\frac{1}{2}}}\left(\frac{\partial x'}{\partial \xi'}\boldsymbol{i} + \frac{\partial y'}{\partial \xi'}\boldsymbol{j}\right), \quad \boldsymbol{e}_\eta = \frac{1}{J^{\frac{1}{2}}}\left(\frac{\partial x'}{\partial \eta'}\boldsymbol{i} + \frac{\partial y'}{\partial \eta'}\boldsymbol{j}\right) \tag{2.5}$$

the velocity components in the two planes are related by

$$U' = \frac{1}{J^{\frac{1}{2}}}\left(u'\frac{\partial y'}{\partial \eta'} - v'\frac{\partial x'}{\partial \eta'}\right), \quad V' = \frac{1}{J^{\frac{1}{2}}}\left(-u'\frac{\partial y'}{\partial \xi'} + v'\frac{\partial x'}{\partial \xi'}\right).$$

Let the stream function $\psi'(x', y') = \psi'(\xi', \eta')$ be defined by

$$u' = \frac{\partial \psi'}{\partial y'}, \quad v' = -\frac{\partial \psi'}{\partial x'}; \tag{2.7}$$

then

$$U' = \frac{1}{J^{\frac{1}{2}}}\frac{\partial \psi'}{\partial \eta'}, \quad V' = -\frac{1}{J^{\frac{1}{2}}}\frac{\partial \psi'}{\partial \xi'}. \tag{2.8}$$

In the mapped plane the vorticity equation can be written as

$$\frac{\partial}{\partial t'}\nabla'^2\psi' - \frac{\partial\left(\psi', \frac{1}{J}\nabla'^2\psi'\right)}{\partial(\xi', \eta')} = \nu\nabla'^2\left(\frac{1}{J}\nabla'^2\psi'\right), \quad \eta' > 0, \tag{2.9}$$

where

$$\nabla'^2 \equiv \frac{\partial^2}{\partial \xi'^2} + \frac{\partial^2}{\partial \eta'^2}. \tag{2.10}$$

The following boundary conditions will be imposed on the wall:

$$\psi' = \frac{\partial \psi'}{\partial \eta'} = 0, \quad \eta' = 0, \tag{2.11a, b}$$

and at infinity

$$\frac{\partial \psi'}{\partial \xi'} = 0, \quad \frac{\partial \psi'}{\partial \eta'} = \omega A \cos \omega t', \quad \eta' \sim \infty. \tag{2.12a, b}$$

It is convenient to begin with the following normalization which is appropriate for the Stokes layer near the ripple surface:

$$\psi = \frac{k\psi'}{A\omega\sigma} = \frac{\psi'}{A\omega\delta}, \quad \xi = k\xi', \quad \eta = \frac{k\eta'}{\sigma} = \frac{\eta'}{\delta}, \quad t = \omega t', \tag{2.13}$$

where $\delta = (\nu/\omega)^{\frac{1}{2}}$. Equations (2.9)–(2.12) then become

$$\frac{\partial}{\partial t}\nabla^2\psi - \alpha\frac{\partial\left(\psi, \frac{1}{J}\nabla^2\psi\right)}{\partial(\xi,\eta)} = \nabla^2\left(\frac{1}{J}\nabla^2\psi\right), \quad \eta > 0, \tag{2.14}$$

$$\psi = \frac{\partial\psi}{\partial\eta} = 0, \quad \eta = 0, \tag{2.15a, b}$$

$$\frac{\partial\psi}{\partial\xi} = 0, \quad \frac{\partial\psi}{\partial\eta} = \cos t, \quad \eta \sim \infty, \tag{2.16a, b}$$

where

$$\nabla^2 \equiv \sigma^2\frac{\partial^2}{\partial\xi^2} + \frac{\partial^2}{\partial\eta^2} \tag{2.17}$$

is a distorted Laplacian operator, and

$$J = 1 - 2\epsilon\cos\xi\,\mathrm{e}^{-\sigma\eta} + \epsilon^2\,\mathrm{e}^{-2\sigma\eta}. \tag{2.18}$$

The three dimensionless parameters α, ϵ and σ have already been defined in §1. Equations (2.14)–(2.18) will be the basis of analysis in §§3–6. Our basic assumptions will be that $\sigma \ll 1$ and that either α or ϵ is small. More specifically we set $\sigma \leqslant O(\alpha) \ll 1$, $\epsilon = O(1)$ in Case (i), and $\sigma \leqslant O(\epsilon\alpha)^{\frac{1}{2}} \ll 1$, $\alpha = O(1)$ in Case (ii).

3. Case (i). Weak oscillations but finite ripple slope: $\alpha \ll 1$, $\epsilon = O(1)$. The Stokes layer

This is a direct extension of the classical problem of an isolated cylinder in an oscillating fluid. We proceed by first examining the Stokes layer and then the outer layer of convective inertia.

Since $\alpha \ll 1$ we introduce expansions in powers of α:

$$\psi = \psi_0 + \alpha\psi_1 + \alpha^2\psi_2 + \ldots \tag{3.1}$$

and

$$J = \tilde{J} + \alpha\left[2\epsilon\cos\xi\left(\frac{\sigma}{\alpha}\eta\right) - 2\epsilon^2\left(\frac{\sigma}{\alpha}\eta\right)\right] + O(\alpha^2), \tag{3.2}$$

where

$$\tilde{J} = 1 - 2\epsilon\cos\xi + \epsilon^2. \tag{3.3}$$

To the leading order, $O(\alpha^0)$, (2.14) and (2.15) give

$$\frac{\partial^2}{\partial\eta^2}\left[\frac{\partial\psi_0}{\partial t} - \frac{1}{\tilde{J}}\frac{\partial^2\psi_0}{\partial\eta^2}\right] = 0, \tag{3.4}$$

$$\psi_0 = \frac{\partial\psi_0}{\partial\eta} = 0, \quad \eta = 0. \tag{3.5}$$

At infinity only (2.16*b*) can be satisfied:

$$\frac{\partial\psi_0}{\partial\eta} = \cos t, \quad \eta \sim \infty. \tag{3.6}$$

In this boundary-value problem the coordinate ξ is only a parameter. The solution is simply that of Stokes boundary layer over a plane:

$$\psi_0 = \tfrac{1}{2}\mathrm{e}^{\mathrm{i}t}\left[\eta + \frac{1}{\tilde{\gamma}}(1 - \mathrm{e}^{\tilde{\gamma}\eta})\right] + *, \tag{3.7}$$

where
$$\tilde{\gamma} = \frac{-1-\mathrm{i}}{\sqrt{2}} \tilde{J}^{\frac{1}{2}}. \tag{3.8}$$

At the outer edge of the Stokes layer this solution yields

$$\psi_0 = [\cos t]\eta + \left[\frac{1}{2\tilde{\gamma}} \mathrm{e}^{\mathrm{i}t} + *\right], \quad \eta \sim \infty. \tag{3.9}$$

The second term implies that there is vertical transport to and from the Stokes boundary layer, which will induce a potential flow outside the Stokes layer.

At the next order, $O(\alpha)$, the governing equation is

$$\begin{aligned}\frac{\partial^2}{\partial\eta^2}\left[\frac{\partial\psi_1}{\partial t} - \frac{1}{\tilde{J}}\frac{\partial^2\psi_1}{\partial\eta^2}\right] &= \frac{\partial\left(\psi_0, \frac{1}{\tilde{J}}\partial^2\psi_0/\partial\eta^2\right)}{\partial(\xi,\eta)} - \frac{1}{\tilde{J}^2}(2\epsilon\cos\xi - 2\epsilon^2)\frac{\sigma}{\alpha}\frac{\partial^2}{\partial\eta^2}\left(\eta\frac{\partial^2\psi_0}{\partial\eta^2}\right) \\ &= \frac{\epsilon\sin\xi}{\tilde{J}}\left[\frac{\tilde{\gamma}}{2\tilde{J}}\mathrm{e}^{(\tilde{\gamma}+\tilde{\gamma}^*)\eta} + \frac{1}{2(2\tilde{J})^{\frac{1}{2}}}\mathrm{e}^{\tilde{\gamma}\eta} + \tfrac{1}{4}\mathrm{i}\eta\,\mathrm{e}^{\tilde{\gamma}\eta}\right] + * \\ &\quad + \frac{\sigma}{\alpha}\frac{\mathrm{i}}{\tilde{J}}(\epsilon\cos\xi - \epsilon^2)(\tilde{\gamma}\eta\,\mathrm{e}^{\tilde{\gamma}\eta} + 2\mathrm{e}^{\tilde{\gamma}\eta})\,\mathrm{e}^{\mathrm{i}t} + * \\ &\quad + \frac{\mathrm{i}\epsilon\sin\xi}{4\tilde{J}}\eta\,\mathrm{e}^{\tilde{\gamma}\eta}\mathrm{e}^{2\mathrm{i}t} + *.\end{aligned} \tag{3.10}$$

The solution consists of zeroth, first and second harmonics in time. On the ripple surface $\eta = 0$, the boundary conditions (2.15a, b) still apply. But at $\eta \sim \infty$, it is necessary to relax (2.16), for the sake of the zeroth harmonic, to

$$\frac{\partial^2\psi_1}{\partial\eta^2} = 0. \tag{3.11}$$

As a consequence ψ_1 and $\partial\psi_1/\partial\xi$ will grow linearly in η, and this must be remedied by adding the outer layer later. The solution is now given as

$$\begin{aligned}\psi_1 = \frac{\epsilon\sin\xi}{\tilde{J}}\Bigg\{ &-\frac{\tilde{\gamma}}{8\tilde{J}^2}[\mathrm{e}^{(\tilde{\gamma}+\tilde{\gamma}^*)\eta} - (\tilde{\gamma}+\tilde{\gamma}^*)\eta - 1] + \frac{1}{(2\tilde{J})^{\frac{3}{2}}}(\mathrm{e}^{\tilde{\gamma}\eta} - \tilde{\gamma}\eta - 1) \\ &+ \frac{\mathrm{i}}{4\tilde{J}}\left(\eta\,\mathrm{e}^{\tilde{\gamma}\eta} - \frac{4}{\tilde{\gamma}}\mathrm{e}^{\tilde{\gamma}\eta} + 3\eta + \frac{4}{\tilde{\gamma}}\right)\Bigg\} + * \\ &- \frac{\sigma}{\alpha}\frac{1}{4\tilde{J}}(\epsilon\cos\xi - \epsilon^2)\left(\eta^2\,\mathrm{e}^{\tilde{\gamma}\eta} - \frac{1}{\tilde{\gamma}}\eta\,\mathrm{e}^{\tilde{\gamma}\eta} + \frac{1}{\tilde{\gamma}^2}\mathrm{e}^{\tilde{\gamma}\eta} - \frac{1}{\tilde{\gamma}^2}\right)\mathrm{e}^{\mathrm{i}t} + * \\ &- \frac{\mathrm{i}\epsilon\sin\xi}{4\tilde{J}^2}\left[\eta\,\mathrm{e}^{\tilde{\gamma}\eta} - \frac{1}{\sqrt{2}\tilde{\gamma}}(\mathrm{e}^{\sqrt{2}\tilde{\gamma}\eta} - 1)\right]\mathrm{e}^{2\mathrm{i}t} + *.\end{aligned} \tag{3.12}$$

From this we obtain at the outer limit of the Stokes layer,

$$\psi_1 = \left[\frac{3\epsilon}{4\tilde{J}^2}\sin\xi\right]\eta + \left[\frac{5\sqrt{2}}{8}\frac{\epsilon\sin\xi}{\tilde{J}^{\frac{3}{2}}} + \frac{\sigma}{\alpha}\frac{1}{4\mathrm{i}\tilde{J}^2}(\epsilon\cos\xi - \epsilon^2)\mathrm{e}^{\mathrm{i}t} + * - \frac{\mathrm{i}\epsilon\sin}{4\tilde{J}^2}\frac{1}{\sqrt{2}\tilde{\gamma}}\mathrm{e}^{2\mathrm{i}t} + *\right]. \tag{3.13}$$

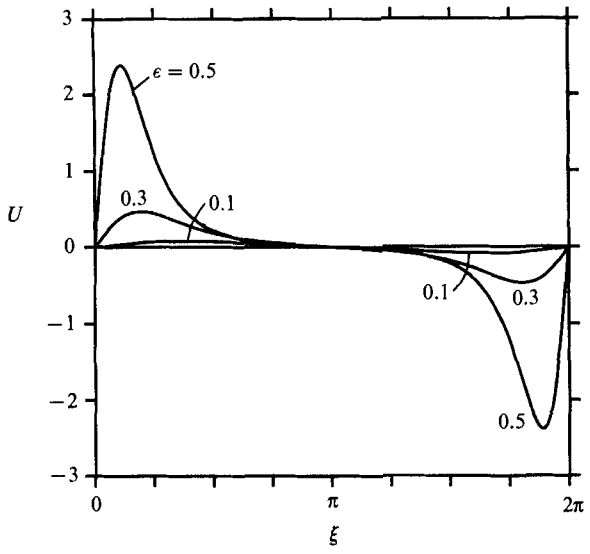

FIGURE 1. Tangential component of induced streaming velocity at the outer edge of a Stokes layer.

The first term proportional to η implies a steady tangential streaming velocity at $O(\alpha)$,

$$\left.\frac{\partial \psi_1}{\partial \eta}\right|_{\infty} = \frac{3\epsilon}{4\tilde{J}^2}\sin\xi \tag{3.14}$$

In figure 1 we plot the tangential component of the induced streaming velocity $U = \tilde{J}^{-\frac{1}{2}}(\partial\psi_1/\partial\eta)|_{\infty}$ in the mapped plane as a function of ξ and ϵ. As the ripple slope ϵ increases, the magnitude of the streaming increases and its peak migrates towards the crest ($\xi = 0, 2\pi$).

The steady Eulerian streaming inside the Stokes layer, given by the zeroth harmonic of (3.12), is plotted in figure 2 in the dimensionless plane of kx' and ky'. To examine the effect of ripple slope we vary ϵ from 0.1 to 0.5 and keep σ at fixed value ($= 0.03$). In all cases there is a pair of vortices between adjacent crests, and the streaming near the ripple surface is directed from a trough to a crest. These vortices become stronger and are squeezed towards crests as the ripple slope increases. Another pair of half-vortices is stacked above the lower pair. These correspond to the lower part of the outer layer to be examined in the next section.

4. Case (i). The outer layer of convective inertia

By requiring that convective inertia and viscous diffusion are comparable in the induced streaming, it can be shown that there must be another layer which lies above, and is $O(1/\alpha)$ times as thick as, the Stokes layer. Therefore we introduce the following normalization:

$$\tilde{\psi} = \alpha\psi, \quad \tilde{\eta} = \alpha\eta \tag{4.1}$$

so that the vorticity equation becomes

$$\frac{\partial}{\partial t}\nabla^2\tilde{\psi} - \alpha\frac{\partial\left(\tilde{\psi}, \frac{1}{J}\tilde{\nabla}^2\tilde{\psi}\right)}{\partial(\xi,\tilde{\eta})} = \alpha^2\tilde{\nabla}^2\left(\frac{1}{J}\tilde{\nabla}^2\tilde{\psi}\right), \tag{4.2}$$

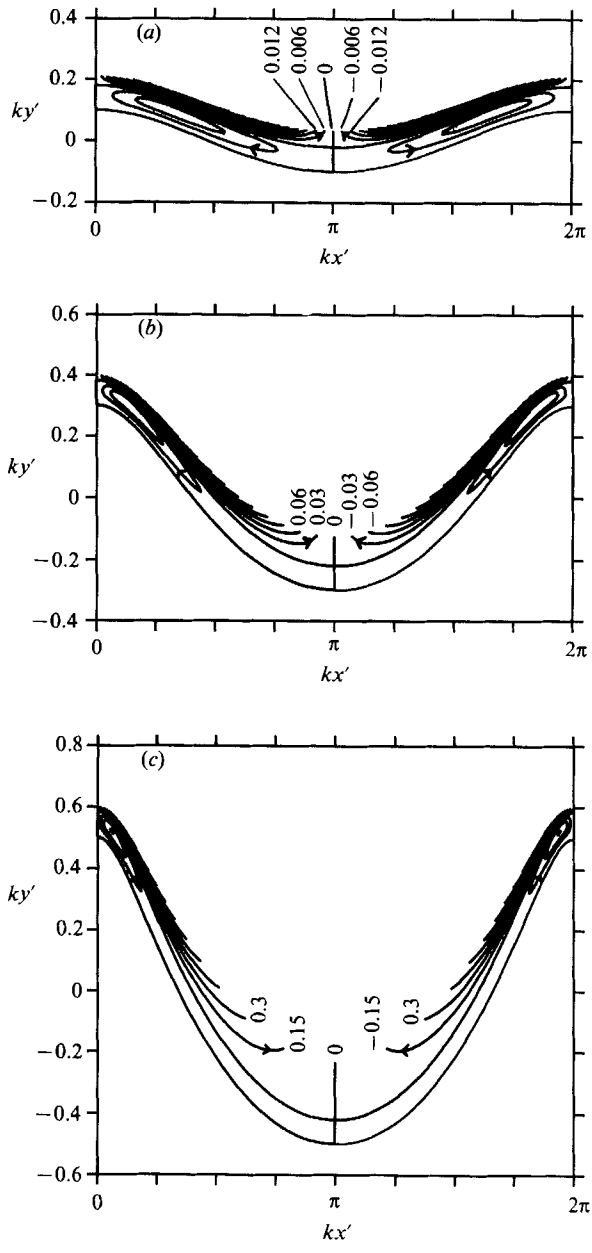

FIGURE 2. Stream-function contours of Eulerian streaming in a Stokes layer. Numbers adjacent to the streamlines represent the values of ψ_1. The vertical scale is stretched by a factor of 4. $\sigma = 0.03$. (*a*) $\epsilon = 0.1$, $\Delta\psi_1 = 0.006$; (*b*) $\epsilon = 0.3$, $\Delta\psi_1 = 0.03$; (*c*) $\epsilon = 0.5$, $\Delta\psi_1 = 0.15$.

where
$$J = 1 - 2\epsilon\cos\xi\exp\left(-\frac{\sigma}{\alpha}\tilde{\eta}\right) + \epsilon^2\exp\left(-2\frac{\sigma}{\alpha}\tilde{\eta}\right), \tag{4.3}$$

and
$$\tilde{\nabla}^2 = \frac{\partial^2}{\partial\tilde{\eta}^2} + \frac{\sigma^2}{\alpha^2}\frac{\partial^2}{\partial\xi^2} \tag{4.4}$$

is a rescaled Laplacian. It is further assumed that $\sigma/\alpha \leqslant O(1)$. The boundary

conditions at $\tilde{\eta} = 0$ are determined by requiring that the stream function and the tangential velocity are matched with the Stokes layer at each order. We now expand

$$\tilde{\psi} = \tilde{\eta}\cos t + \alpha\tilde{\psi}_1 + \alpha^2\psi_2 + \dots, \tag{4.5}$$

where the first term is matched with the first term of (3.9). At the next order, $O(\alpha^1)$, we find from (4.2)

$$\frac{\partial}{\partial t}\tilde{\nabla}^2\tilde{\psi}_1 = 0. \tag{4.6}$$

The Stokes-layer solutions which should be matched at this order are the second term of (3.9) and the first term of (3.13). Therefore the solution must be composed of both zeroth and first harmonics:

$$\tilde{\psi}_1 = \tilde{\psi}_1^0(\xi, \tilde{\eta}) + [\tilde{\psi}_1^1(\xi, \tilde{\eta})\,e^{it} + *]. \tag{4.7}$$

From (4.6) the first harmonic is a potential flow governed by the following Laplace equation:

$$\tilde{\nabla}^2\tilde{\psi}_1^1 = 0, \quad \tilde{\eta} > 0. \tag{4.8}$$

The boundary condition at $\tilde{\eta} = 0$ follows from the second term of (3.9),

$$\tilde{\psi}_1^1 = \frac{1}{2\tilde{\gamma}}, \quad \tilde{\eta} = 0; \tag{4.9}$$

we also impose

$$\frac{\partial\tilde{\psi}_1^1}{\partial\tilde{\eta}} = 0, \quad \tilde{\eta} \sim \infty. \tag{4.10}$$

The forcing term in (4.9) can be expanded as a Fourier series in ξ:

$$\frac{1}{2\tilde{\gamma}} = \frac{1}{2\gamma J_{\frac{1}{2}}} = \frac{1}{2\gamma}\sum_0^\infty a_n \cos n\xi, \tag{4.11}$$

where the Fourier coefficients are proportional to hypergeometric functions

$$\left.\begin{aligned} a_0 &= F(\tfrac{1}{2}, \tfrac{1}{2}, 1; \epsilon^2), \\ a_n &= 2\frac{\epsilon^n \Gamma(n+\frac{1}{2})}{n!\,\Gamma(\frac{1}{2})} F(\tfrac{1}{2}, n+\tfrac{1}{2}, n+1; \epsilon^2), \quad n \neq 0 \end{aligned}\right\} \tag{4.12}$$

and

$$\gamma = \frac{-1-i}{\sqrt{2}}. \tag{4.13}$$

It follows readily that

$$\tilde{\psi}_1^1 = \frac{1}{2\gamma}\left[a_0 + \sum_1^\infty a_n \exp\left(-n\frac{\sigma}{\alpha}\tilde{\eta}\right)\cos n\xi\right]. \tag{4.14}$$

This solution gives rise to the following normal derivative at the bottom:

$$\frac{\partial\tilde{\psi}_1^1}{\partial\tilde{\eta}} = \frac{1}{2\gamma}\sum_1^\infty -n\frac{\sigma}{\alpha}a_n \cos n\xi, \quad \tilde{\eta} = 0. \tag{4.15}$$

The Stokes-layer solution (3.12) must now be adjusted by adding the following term:

$$\frac{1}{2\gamma}\left[\sum_1^\infty -n\frac{\sigma}{\alpha}a_n \cos n\xi\right]\left[\eta + \frac{1}{\tilde{\gamma}}(1 - e^{\tilde{\gamma}\eta})\right]e^{it} + *, \tag{4.16}$$

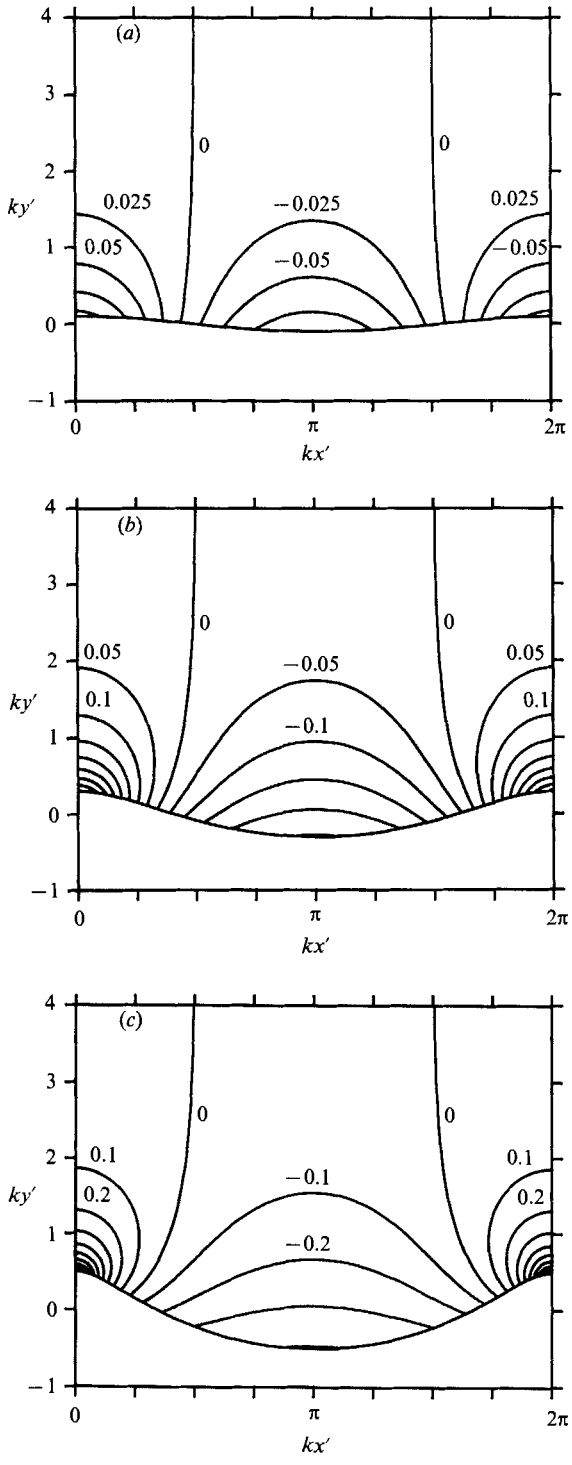

FIGURE 3. Stream-function contours of the first harmonic in a Stuart layer. Numbers adjacent to the streamlines represent the values of $\phi - a_0$. (*a*) $\epsilon = 0.1$, $\Delta\phi = 0.025$; (*b*) $\epsilon = 0.3$, $\Delta\phi = 0.05$; (*c*) $\epsilon = 0.5$, $\Delta\phi = 0.1$.

which satisfies the homogeneous equation of (3.10). The first harmonic in the outer layer can be now written as

$$\tilde{\psi}_1^1 e^{it} + * = \left(\frac{e^{it}}{2\gamma} + *\right)\phi = -\cos(t - \tfrac{1}{4}\pi)\,\phi, \tag{4.17}$$

where

$$\phi(\xi, \tilde{\eta}) = a_0 + \sum_1^\infty a_n \exp\left(-n\frac{\sigma}{\alpha}\tilde{\eta}\right)\cos n\xi \tag{4.18}$$

is the spatial structure of the first harmonic. In figure 3 we plot $\phi(\xi, \tilde{\eta})$ in the kx' *vs.* ky' plane for $\epsilon = 0.1$, 0.3, and 0.5. There is transport of fluid to and from the Stokes layer; this transport becomes more intense around a crest for a steeper ripple.

The zeroth harmonic which represents steady streaming satisfies (4.6) trivially. Further information must come from higher orders. At $O(\alpha^2)$ the vorticity equation gives

$$\frac{\partial}{\partial t}\tilde{\nabla}^2\tilde{\psi}_2 + \cos t\frac{\partial}{\partial \xi}\left(\frac{1}{J}\tilde{\nabla}^2\tilde{\psi}_1\right) = 0; \tag{4.19}$$

hence

$$\tilde{\nabla}^2\tilde{\psi}_2 = -\sin t\frac{\partial}{\partial \xi}\left(\frac{1}{J}\tilde{\nabla}^2\tilde{\psi}_1\right) + f(\xi, \tilde{\eta}), \tag{4.20}$$

where f may be determined at a higher order but will not be needed for our purposes. At $O(\alpha^3)$ we get from (4.2)

$$\frac{\partial}{\partial t}\tilde{\nabla}^2\tilde{\psi}_3 + \cos t\frac{\partial}{\partial \xi}\left(\frac{1}{J}\tilde{\nabla}^2\tilde{\psi}_2\right) - \frac{\partial\left(\tilde{\psi}_1, \frac{1}{J}\tilde{\nabla}^2\tilde{\psi}_1\right)}{\partial(\xi, \tilde{\eta})} = \tilde{\nabla}^2\left(\frac{1}{J}\tilde{\nabla}^2\tilde{\psi}_1\right). \tag{4.21}$$

Upon inserting (4.7) and (4.20), taking the time average of (4.21) and using (4.8), we finally obtain the governing equation for $\tilde{\psi}_1^0$:

$$-\frac{\partial\left(\tilde{\psi}_1^0, \frac{1}{J}\tilde{\nabla}^2\tilde{\psi}_1^0\right)}{\partial(\xi, \tilde{\eta})} = \tilde{\nabla}^2\left(\frac{1}{J}\tilde{\nabla}^2\tilde{\psi}_1^0\right). \tag{4.22}$$

The boundary conditions at the bottom follow from the second term of (3.9) and the first term of (3.13) (or (3.14)):

$$\tilde{\psi}_1^0 = 0, \quad \tilde{\eta} = 0, \tag{4.23}$$

$$\frac{\partial\tilde{\psi}_1^0}{\partial\tilde{\eta}} = \frac{3\epsilon}{4\tilde{J}^2}\sin\xi, \quad \tilde{\eta} = 0. \tag{4.24}$$

At infinity we expect the steady streaming to vanish, and impose

$$\frac{\partial\tilde{\psi}_1^0}{\partial\xi} = \frac{\partial\tilde{\psi}_1^0}{\partial\tilde{\eta}} = 0, \quad \tilde{\eta} \sim \infty. \tag{4.25}$$

Thus the steady streaming in the outer layer is governed by the steady Navier–Stokes equations including convective inertia, and is driven at the bottom by a spatially periodic steady tangential velocity. If $\sigma/\alpha \ll 1$, the ξ-derivative in the Laplacian operator $\tilde{\nabla}^2$ can be omitted; (4.22) can be integrated once to yield the Blasius boundary-layer equation. This limit was first shown by Stuart (1963, 1966) and Riley (1965) for a circular cylinder. However, when there are two boundary layers converging toward each other over a ripple trough, the flow must then turn away from the wall as a jet; the Blasius approximation breaks down. To treat this transition into a jet new remedies are needed, as described by Davidson & Riley

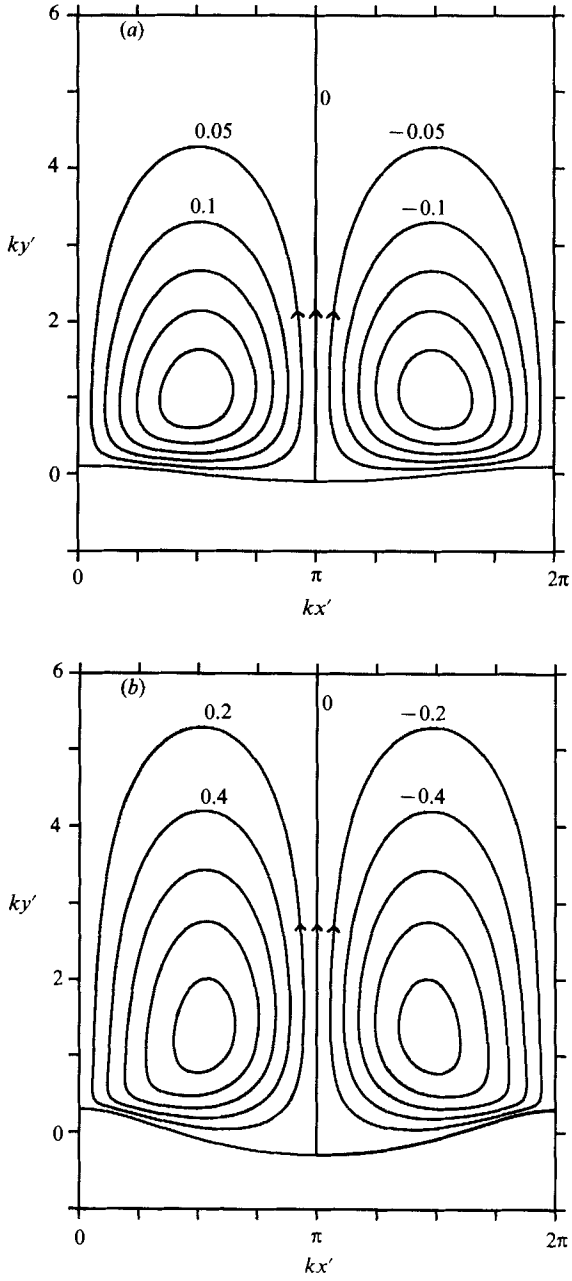

FIGURE 4(a,b). For caption see facing page.

(1972) for the circular cylinder. Since the fuller equation (4.22) can be solved by existing numerical means, the Blasius limit will not be discussed here. This approach, with boundary conditions imposed at a finite height (instead of (4.25)) has been used before by Haddon & Riley (1983).

Because the boundary condition (4.24) is sinusoidal in ξ we employ the spectral method and expand $\tilde{\psi}_1^0$ as a Fourier series

$$\tilde{\psi}_1^0 = \sum_1^\infty b_n \sin n\xi. \tag{4.26}$$

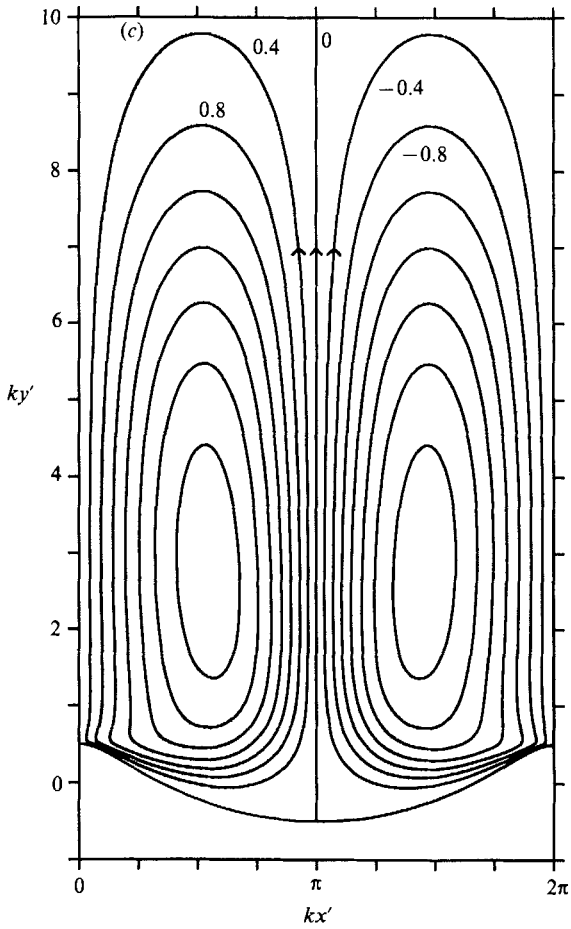

FIGURE 4. Stream-function contours of Eulerian streaming in a Stuart layer. Numbers adjacent to the streamlines represent the values of $\tilde{\psi}_1^0$. $\alpha/\sigma = 10$. (*a*) $\epsilon = 0.1$, $\Delta\tilde{\psi}_1^0 = 0.05$; (*b*) $\epsilon = 0.3$, $\Delta\tilde{\psi}_1^0 = 0.2$; (*c*) $\epsilon = 0.5$, $\Delta\tilde{\psi}_1^0 = 0.4$.

An infinite set of nonlinear ordinary differential equations coupling the functions $b_n(\tilde{\eta})$ results. After truncation at finite terms the equations are approximated by finite differences in $\tilde{\eta}$ with smaller grids for smaller $\tilde{\eta}$. The difference equations are solved by Newton–Ralphson iteration. Since the method is known and has been employed before in similar mathematical problems (Caponi *et al.* 1982), details are omitted here. This numerical task is of course far simpler than that needed to solve the exact transient Navier–Stokes equations.

We show in figure 4 the steady vortices in the outer layer in the dimensionless plane of kx' and ky'. Again we vary ϵ from 0.1 to 0.5 and keep σ and α at fixed values ($\alpha/\sigma = 10$). In all cases there is a pair of counter-rotating vortices between two adjacent ripple crests. The size of these vortices is of the same order as the ripple wavelength. As ϵ increases the vortices grow larger in size and stronger in magnitude. The flow near the crest is intensified by the forcing from the Stokes layer. The effects of increasing $R = (\alpha/\sigma)^2$ by either increasing α or decreasing σ are similar to those in §6. In particular as R increases the upward flow from the trough intensifies to become jet-like. No plots are shown here. In the calculations of Haddon & Riley, the steady

	Parameter regime	Reynolds number
Lyne (1971) (i)	$\alpha \ll 1,\ \epsilon/\sigma \ll 1$	$\epsilon\alpha^2/\sigma^2 \ll 1$
Lyne (1971) (ii)	$\alpha \gg 1,\ \epsilon/\sigma \ll 1,\ \sigma \ll 1$	$\epsilon\alpha/\sigma^2 \ll 1$
Sleath (1974*a*)	$\alpha \ll 1,\ \epsilon \ll 1$	$\epsilon\alpha^2/\sigma^2 \ll 1$
Kaneko & Honji (1979)	$\alpha \ll 1,\ \epsilon/\sigma \leqslant O(1)$	$\epsilon\alpha^2/\sigma^2 \ll 1$
Matsunaga *et al.* (1981)	$\alpha \ll 1,\ \epsilon = O(1),$	$\epsilon\alpha^2/\sigma^2 \ll 1$
Vittori (1989)	$\alpha = O(1),\ \epsilon/\sigma \ll 1$	$\epsilon\alpha/\sigma^2 \ll 1$
This study, Case (i)	$\alpha \ll 1,\ \epsilon = O(1)$	$\epsilon\alpha^2/\sigma^2 \geqslant O(1)$
This study, Case (ii)	$\alpha = O(1),\ \epsilon \ll 1$	$\epsilon\alpha/\sigma^2 \geqslant O(1)$

TABLE 1. Summary of regimes of validity of various theories

streaming cells outside the Stokes layer on a flat bed under standing waves has a finite height because the horizontal wavelength is comparable with the water depth. Therefore the vertical jets are strongly inhibited by the free surface; this situation is different from ours where the water depth is much greater than the ripple wavelength.

Combining figures 2 and 4, we obtain the whole picture of steady streaming consisting of two pairs of vortices; the larger pair stacked above the smaller. This result is qualitatively similar to those by Lyne (1971) for small ϵ and α, and extended by Kaneko & Honji (1979) and Matsunaga *et al.* (1981) for finite ϵ. However, their theory is derived for a different regime of a much thicker Stokes layer. In table 1, we summarize the regimes of validity of these theories, noting in particular the constraints on the Reynolds number which is defined differently in different situations.

So far the solutions have been obtained up to $O(\alpha)$ both in the Stokes layer and in the outer layer of convective inertia. Terms in the second pair of brackets on the right-hand side of (3.13), which correspond to the normal velocity at the outer edge of the Stokes layer, should be matched to an $O(\alpha^2)$ solution $\tilde{\psi}_2$ in the outer layer. Because its effect is always of $O(\alpha^2)$, we do not pursue it here.

5. Case (ii). Strong oscillations but small ripple slope: $\alpha = O(1), \epsilon \ll 1$. The Stokes boundary layer

In this and the next section focus will be on the case of finite Keulegan–Carpenter number.

5.1. *Analysis*

First it is advantageous to transform from (2.1) to the coordinate system oscillating with the ambient fluid:

$$\tilde{\xi} = \xi - \alpha \sin t = k(\xi' - A \sin \omega t'). \tag{5.1}$$

All other normalizations in (2.13) are kept. The vorticity equation in Stokes-layer coordinates now become

$$\left(\frac{\partial}{\partial t} - \alpha \cos t \frac{\partial}{\partial \tilde{\xi}}\right) \nabla^2 \psi - \alpha \frac{\partial\left(\psi, \frac{1}{J}\nabla^2\psi\right)}{\partial(\tilde{\xi}, \eta)} = \nabla^2\left(\frac{1}{J}\nabla^2\psi\right) \tag{5.2}$$

where the Laplacian operator is still given by (2.17) except that ξ must be replaced by $\tilde{\xi}$. The Jacobian now takes the form

$$J = 1-2\epsilon\cos(\tilde{\xi}+\alpha\sin t)\,\mathrm{e}^{-\sigma\eta}+\epsilon^2\,\mathrm{e}^{-2\sigma\eta}. \tag{5.3}$$

The boundary conditions (2.15) and (2.16) of course remain valid.

We begin by substituting the following expansions:

$$\psi = \psi_0+\epsilon\psi_1+O(\epsilon^{\frac{3}{2}}), \tag{5.4}$$

$$\frac{1}{J} = 1+2\epsilon\cos(\tilde{\xi}+\alpha\sin t)+O(\epsilon^{\frac{3}{2}}), \tag{5.5}$$

into (5.2) and the boundary conditions (2.15) and (2.16).

At $O(\epsilon^0)$, the solution of ψ_0 is

$$\psi_0 = \tfrac{1}{2}\mathrm{e}^{\mathrm{i}t}\left[\eta+\frac{1}{\gamma}(1-\mathrm{e}^{\gamma\eta})\right]+*, \tag{5.6}$$

where γ is given by (4.13). Unlike (3.7), the solution here is independent of $\tilde{\xi}$. At the outer edge of the Stokes layer this solution yields

$$\psi_0 = [\cos t]\eta+\left[\frac{1}{2\gamma}\mathrm{e}^{\mathrm{i}t}+*\right], \quad \eta\sim\infty, \tag{5.7}$$

where the second term now does not induce any vertical velocity.

At $O(\epsilon)$ the perturbation equation for ψ_1 is

$$\left(\frac{\partial}{\partial t}-\alpha\cos t\frac{\partial}{\partial\tilde{\xi}}\right)\frac{\partial^2\psi_1}{\partial\eta^2}+\alpha\frac{\partial\psi_0}{\partial\eta}\frac{\partial^3\psi_1}{\partial\tilde{\xi}\partial\eta^2}-\alpha\frac{\partial^3\psi_0}{\partial\eta^3}\frac{\partial\psi_1}{\partial\tilde{\xi}}-\frac{\partial^4\psi_1}{\partial\eta^4}$$
$$= \alpha\frac{\partial(\psi_0, 2\cos(\tilde{\xi}+\alpha\sin t)\,\partial^2\psi_0/\partial\eta^2)}{\partial(\tilde{\xi},\eta)}+2\cos(\tilde{\xi}+\alpha\sin t)\frac{\partial^4\psi_0}{\partial\eta^4}. \tag{5.8}$$

The details of the right-hand side can be worked out to be

$$= 2\alpha\sin(\tilde{\xi}+\alpha\sin t)\frac{\partial\psi_0}{\partial\eta}\frac{\partial^2\psi_0}{\partial\eta_2}+2\cos(\tilde{\xi}+\mathrm{a}\sin t)\frac{\partial^4\psi_0}{\partial\eta^4}$$

$$= \frac{\alpha}{4i}[\mathrm{e}^{\mathrm{i}t}(1-\mathrm{e}^{\gamma\eta})+*][-\gamma\mathrm{e}^{\mathrm{i}t}\mathrm{e}^{\gamma\eta}+*]\sum_{-\infty}^{\infty}[\mathrm{e}^{\mathrm{i}\tilde{\xi}}-(-)^n\mathrm{e}^{-\mathrm{i}\tilde{\xi}}]\mathrm{e}^{\mathrm{i}nt}J_n(\alpha)$$

$$+\tfrac{1}{2}[\mathrm{e}^{\mathrm{i}t}(-\mathrm{i}\gamma)\mathrm{e}^{\gamma\eta}+*]\sum_{-\infty}^{\infty}(\mathrm{e}^{\mathrm{i}\tilde{\xi}}+(-)^n\mathrm{e}^{-\mathrm{i}\tilde{\xi}})\mathrm{e}^{\mathrm{i}nt}J_n(\alpha)$$

$$= \sum_{-\infty}^{\infty}\mathrm{e}^{\mathrm{i}nt}[\mathrm{e}^{\mathrm{i}\tilde{\xi}}-(-)^n\mathrm{e}^{-\mathrm{i}\tilde{\xi}}]\left\{\frac{\alpha}{4\mathrm{i}}(1-\mathrm{e}^{\gamma\eta})[-\gamma\mathrm{e}^{\gamma\eta}J_{n-2}(\alpha)-\gamma^*\mathrm{e}^{\gamma^*\eta}J_n(\alpha)]\right.$$

$$+\frac{\alpha}{4\mathrm{i}}(1-\mathrm{e}^{\gamma^*\eta})[-\gamma\mathrm{e}^{\gamma\eta}J_n(\alpha)-\gamma^*\mathrm{e}^{\gamma^*\eta}J_{n+2}(\alpha)]$$

$$\left.-\tfrac{1}{2}\mathrm{i}\gamma\mathrm{e}^{\gamma\eta}J_{n-1}(\alpha)+\tfrac{1}{2}\mathrm{i}\gamma^*\mathrm{e}^{\gamma^*\eta}J_{n+1}(\alpha)\right\}, \tag{5.9}$$

where $J_n(\alpha)$ is the Bessel function of order n. Use has been made of the following identities:

$$\sin(\tilde{\xi}+\alpha\sin t) = \sin\tilde{\xi}\cos(\alpha\sin t)+\cos\tilde{\xi}\sin(\alpha\sin t)$$

$$= \left(\sin\tilde{\xi}\sum_{n=\text{even}} - \mathrm{i}\cos\tilde{\xi}\sum_{n=\text{odd}}\right)\mathrm{e}^{\mathrm{i}nt}J_n(\alpha)$$

$$= \frac{1}{2\mathrm{i}}\sum_{-\infty}^{\infty}[\mathrm{e}^{\mathrm{i}\tilde{\xi}}-(-)^n\mathrm{e}^{-\mathrm{i}\tilde{\xi}}]\mathrm{e}^{\mathrm{i}nt}J_n(\alpha) \tag{5.10}$$

and

$$\cos(\tilde{\xi}+\alpha\sin t) = \frac{1}{2}\sum_{-\infty}^{\infty}[\mathrm{e}^{\mathrm{i}\tilde{\xi}}+(-)^n\mathrm{e}^{-\mathrm{i}\tilde{\xi}}]\mathrm{e}^{\mathrm{i}nt}J_n(\alpha). \tag{5.11}$$

The form of the forcing term in (5.9) implies that $\sin\tilde{\xi}$ is multiplied by only even harmonics, while $\cos\tilde{\xi}$ by only odd harmonics, in time.

We now assume that

$$\psi_1 = \sum_{-\infty}^{\infty}\mathrm{e}^{\mathrm{i}nt}(\mathrm{e}^{\mathrm{i}\tilde{\xi}}\psi_{n,1}+\mathrm{e}^{-\mathrm{i}\tilde{\xi}}\psi_{n,-1}). \tag{5.12}$$

For ψ_1 to be real it is necessary that

$$\mathrm{e}^{-\mathrm{i}\tilde{\xi}}\psi^*_{n,1}+\mathrm{e}^{\mathrm{i}\tilde{\xi}}\psi^*_{n,-1} = \mathrm{e}^{\mathrm{i}\tilde{\xi}}\psi_{-n,1}+\mathrm{e}^{-\mathrm{i}\tilde{\xi}}\psi_{-n,-1}. \tag{5.13}$$

Hence $$\psi_{n,-1} = \psi^*_{-n,1} \quad \text{or, equivalently} \quad \psi^*_{n,1} = \psi_{-n,-1}. \tag{5.14}$$

By substituting (5.12) into (5.8) and collecting the coefficients of $\mathrm{e}^{\mathrm{i}nt}\mathrm{e}^{\mathrm{i}\tilde{\xi}}$, we obtain a system of ordinary differential equations for $\psi_{n,1}$:

$$\mathrm{i}n\psi''_{n,1}-\tfrac{1}{2}\mathrm{i}\alpha\,\mathrm{e}^{\gamma\eta}\psi''_{n-1,1}-\tfrac{1}{2}\mathrm{i}\alpha\,\mathrm{e}^{\gamma^*\eta}\psi''_{n+1,1}-\tfrac{1}{2}\alpha\,\mathrm{e}^{\gamma\eta}\psi_{n-1,1}+\tfrac{1}{2}\alpha\,\mathrm{e}^{\gamma^*\eta}\psi_{n+1,1}-\psi''''_{n,1}$$

$$= \frac{\alpha}{4\mathrm{i}}(1-\mathrm{e}^{\gamma\eta})[-\gamma\,\mathrm{e}^{\gamma\eta}J_{n-2}(\alpha)-\gamma^*\mathrm{e}^{\gamma^*\eta}J_n(\alpha)]+\frac{\alpha}{4\mathrm{i}}(1-\mathrm{e}^{\gamma^*\eta})[-\gamma\,\mathrm{e}^{\gamma\eta}J_n(\alpha)-\gamma^*\mathrm{e}^{\gamma^*\eta}J_{n+2}(\alpha)]$$

$$-\tfrac{1}{2}\mathrm{i}\gamma\,\mathrm{e}^{\gamma\eta}J_{n-1}(\alpha)+\tfrac{1}{2}\mathrm{i}\gamma^*\mathrm{e}^{\gamma^*\eta}J_{n+1}(\alpha). \tag{5.15}$$

From the even and odd parity of the forcing term (5.9), a further symmetry relation can be deduced. Let the left-hand side of (5.8) be denoted by

$$\sum_{-\infty}^{\infty}\mathrm{e}^{\mathrm{i}nt}(L_{n,1}\,\mathrm{e}^{\mathrm{i}\tilde{\xi}}-L_{n,-1}\,\mathrm{e}^{-\mathrm{i}\tilde{\xi}}) = \sum_{-\infty}^{\infty}\mathrm{e}^{\mathrm{i}nt}[\cos\tilde{\xi}(L_{n,1}+L_{n,-1})+\mathrm{i}\sin\tilde{\xi}(L_{n,1}-L_{n,-1})], \tag{5.16}$$

where $L_{n,1}$ corresponds to the left-hand side of (5.15). To conform with the parity on the right-hand side of (5.8) (see (5.9)) we must have, for the coefficients on the right of (5.16),

$$L_{n,1}+L_{n,-1} = 0, \quad n = \text{even}; \quad L_{n,1}-L_{n,-1} = 0, \quad n = \text{odd}; \tag{5.17}$$

After inferring the expression for $L_{n,-1}$ from the left-hand side of (5.15) we find

$$L_{n,1}\pm L_{n,-1} = \mathrm{i}n(\psi''_{n,1}\pm\psi''_{n,-1})-\tfrac{1}{2}\alpha(\mathrm{i}\,\mathrm{e}^{\gamma\eta})(\psi''_{n-1,1}\mp\psi''_{n-1,-1})$$

$$-\tfrac{1}{2}\alpha(\mathrm{i}\mathrm{e}^{\gamma^*\eta})(\psi''_{n+1,1}\mp\psi''_{n+1,-1})-\tfrac{1}{2}\alpha\mathrm{e}^{\gamma\eta}(\psi_{n-1,1}\mp\psi_{n-1,-1})$$

$$+\tfrac{1}{2}\alpha\mathrm{e}^{\gamma^*\eta}(\psi_{n+1,1}\mp\psi_{n+1,-1})-(\psi''''_{n,1}\pm\psi''''_{n,-1}). \tag{5.18}$$

Since when n = even, $n\pm1$ = odd and vice versa, we conclude from (5.17) that

$$\psi_{n,1} = -(-)^n\psi_{n,-1}. \tag{5.19}$$

With the help of (5.14) and (5.19), only one quarter of the unknowns of $\psi_{n,1}$ and $\psi_{n,-1}$ needs to be computed.

The boundary conditions (2.15*a*, *b*) imply that

$$\psi_{n,1} = \psi'_{n,1} = 0, \quad \eta = 0. \tag{5.20}$$

The simultaneous differential equations (5.15) are linear but with variable coefficients, and must be solved numerically. The technique used is similar to that of Hall (1978) and combines the asymptotic representation for large η and finite difference approximation for intermediate to small values of η. For large η we drop the exponentially small terms and obtain from (5.15) that

$$\mathrm{i}n\psi''_{n,1} - \psi''''_{n,1} = 0 \tag{5.21}$$

for all $n = \pm 0, 1, 2, \ldots$. For the velocity to be bounded at infinity we take

$$\psi_{0,1} = A_0 + B_0\eta, \quad \psi_{n,1} = A_n + B_n \exp[-(\mathrm{i}n)^{\frac{1}{2}}\eta], \quad n \neq 0 \tag{5.22}$$

where

$$(\mathrm{i}n)^{\frac{1}{2}} = |n|^{\frac{1}{2}}\frac{1+\mathrm{i}}{\sqrt{2}}, \quad n > 0$$

$$= |n|^{\frac{1}{2}}\frac{1-\mathrm{i}}{\sqrt{2}}, \quad n < 0. \tag{5.23}$$

Note that for the zeroth harmonic the horizontal velocity is not required to vanish at infinity.

In view of (5.14) and (5.19) we must have for $n \neq 0$

$$A_{-n} + B_{-n}\exp[-(-\mathrm{i}n)^{\frac{1}{2}}\eta] = -(-)^n\{A_n^* + B_n^*\exp[-(-\mathrm{i}n)^{\frac{1}{2}}\eta]\}. \tag{5.24}$$

Thus
$$A_{-n} = -(-)^n A_n^*, \quad B_{-n} = -(-)^n B_n^*. \tag{5.25}$$

Similarly for $n = 0$ we have
$$A_0 + B_0\eta = -A_0^* - B_0^*\eta \tag{5.26}$$

so that
$$A_0 = -A_0^*, \quad B_0 = -B_0^*. \tag{5.27}$$

Thus A_0 and B_0 are pure imaginary. Physically B_0 corresponds to the tangential induced streaming at the outer edge of Stokes layer.

In computations the series (5.12) is truncated at a large value $n = N$. For $\eta > \eta_M$ (5.22) is used with (5.12) to represent the solution. For $\eta < \eta_M$ the fourth-order Runge–Kutta method is applied to integrate (5.15) downward from η_M. The initial values of the $\psi_{n,1}$ and their derivatives at $\eta = \eta_M$ are expressed in terms of asymptotic representation with unknown coefficients A_n and B_n, which are determined by the boundary conditions at $\eta = 0$.

5.2. *Results and discussion*

After solving for all harmonics we obtain the stream function $\psi_0 + \epsilon\psi_1$ in the entire Stokes layer. At the outer edge of the Stokes layer ψ_1 becomes

$$\psi_1 = [B_0 \mathrm{e}^{\mathrm{i}\tilde{\xi}} + *]\eta + \left\{\sum_{-\infty}^{\infty} A_n \mathrm{e}^{\mathrm{i}nt}[\mathrm{e}^{\mathrm{i}\tilde{\xi}} - (-)^n \mathrm{e}^{-\mathrm{i}\tilde{\xi}}]\right\}, \quad \eta \sim \infty. \tag{5.28}$$

In particular the first term leads to a non-zero steady streaming velocity in the oscillating frame of reference. The corresponding tangential velocity in the mapped plane of $\tilde{\xi}, \eta$ is

$$\langle U\rangle = \left\langle \frac{1}{J^{\frac{1}{2}}}\frac{\partial\psi_1}{\partial\eta}\right\rangle = B_0\mathrm{e}^{\mathrm{i}\tilde{\xi}} + * + O(\epsilon) = C\sin\tilde{\xi} + O(\epsilon), \quad \eta \sim \infty. \tag{5.29}$$

Use has been made of the fact that $B_0 = -\frac{1}{2}\mathrm{i}C$ is imaginary.

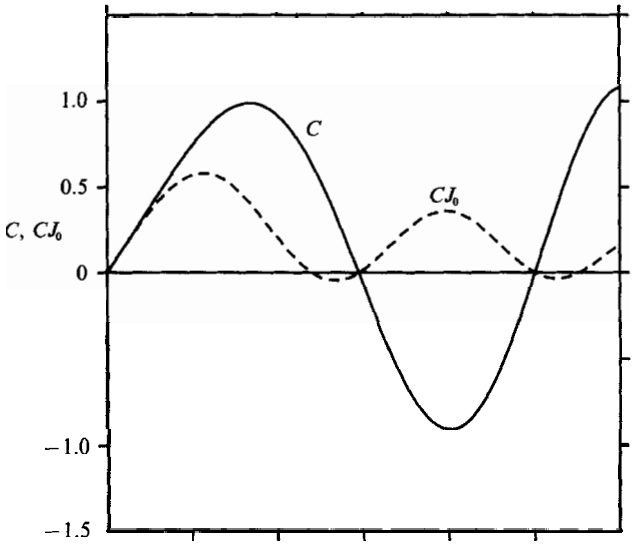

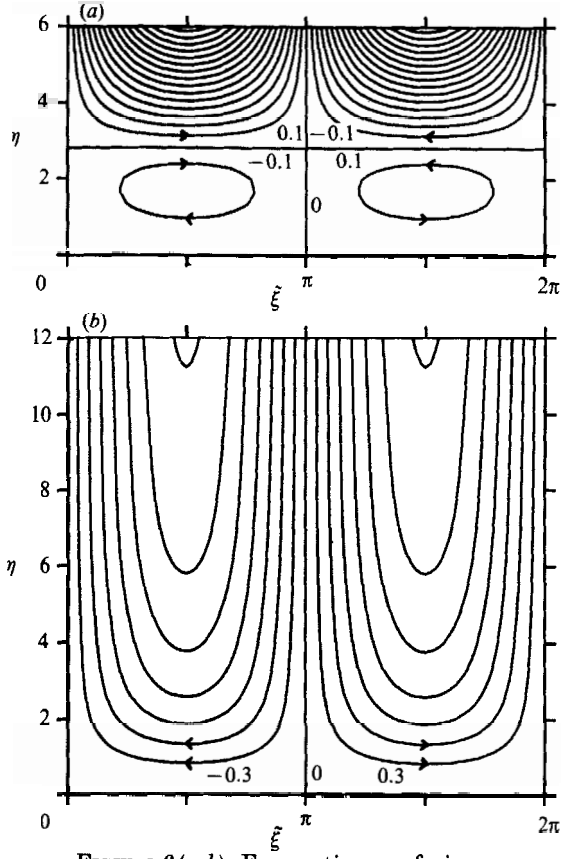

FIGURE 6(*a*,*b*). For caption see facing page.

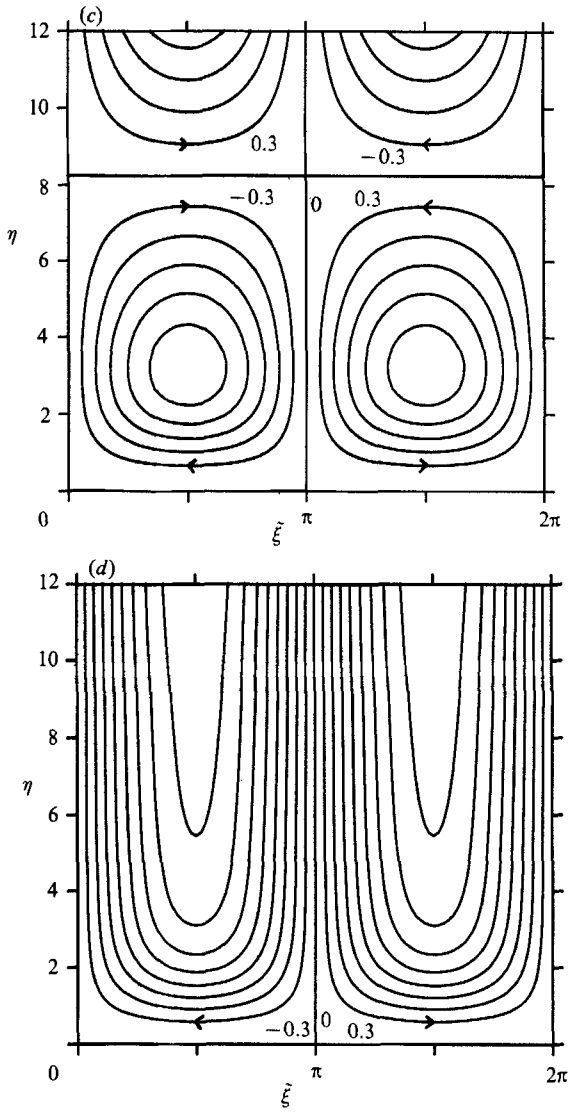

FIGURE 6. Stream-function contours of Eulerian streaming in a Stokes layer. Numbers adjacent to the streamlines represent the values of ψ_1. (*a*) $\alpha = 1.1$, $\Delta\psi_1 = 0.1$; (*b*) $\alpha = 2.7$, $\Delta\psi_1 = 0.3$; (*c*) $\alpha = 4.0$, $\Delta\psi_1 = 0.3$; (*d*) $\alpha = 5.3$, $\Delta\psi_1 = 0.3$.

The amplitude $C(\alpha)$ is plotted in figure 5 as a function of α. Within the computed range of α: $0 < \alpha < 6$, there are two zeros at $\alpha = 2.95$ and 5.0. As a check of accuracy we note that in the limit of $\alpha \ll 1$, $C \to \frac{3}{4}\alpha$ which agrees with (3.14) to the zeroth order in ϵ.

We now transform (5.29) back to the stationary coordinates

$$\langle U \rangle = C \sin(\xi - \alpha \sin t) = \frac{C}{2\mathrm{i}} \sum_{-\infty}^{\infty} (\mathrm{e}^{\mathrm{i}\xi} - (-)^n \mathrm{e}^{-\mathrm{i}\xi}) \mathrm{e}^{-\mathrm{i}nt} J_n(\alpha). \tag{5.30}$$

The zeroth harmonic of (5.30) is the mean Eulerian drift at the outer edge of the Stokes layer as seen by a stationary observer:

$$\langle U \rangle_0 = C(\alpha) J_0(\alpha) \sin \xi, \quad \eta \sim \infty. \tag{5.31}$$

The product CJ_0 is plotted in figure 5 also. It is nearly always positive except for the small intervals $2.4 < \alpha < 2.95$ and $5.0 < \alpha < 5.5$. Thus the Eulerian streaming just outside the Stokes layer is nearly always directed from ripple crests to ripple troughs (from $\xi = 2n\pi$ to $\xi = (2n \pm 1)\pi$).

We shall not discuss the transient aspects of the interior of the Stokes layer, which is given by (5.12) including all the time harmonics. To obtain the Eulerian streaming inside the Stokes layer we first transfer (5.12) back to the stationary frame of reference and then take the time average. Sample results are shown in figure 6. For $\alpha = 2.7$ and 5.3 when CJ_0 has negative maxima, there is only one cell between a ripple crest and its adjacent trough. However for $\alpha = 1.1$ and 4 when CJ_0 has positive maxima, there are two cells stacked up vertically. Near the ripple surface, the streaming is always directed from a trough to a crest, implying that mass transport by waves tends to enhance the growth of sand ripples. This qualitative trend has been found by Sleath (1974*b*, 1975) for a different range of parameters.

6. Case (ii). The outer layer of convective inertia

6.1. *Analysis*

As was shown in §5, while both transient and steady motions are present inside the Stokes boundary layer of thickness $O(\delta)$, an oscillating observer sees only a steady streaming, at the outer edge. Since the tangential streaming velocity is of $O(\epsilon)$, balance between convective inertia and viscous diffusion requires the presence of an outer layer $O(1/(\alpha\epsilon)^{\frac{1}{2}})$ times as thick as the Stokes layer. We therefore introduce the following renormalization which is convenient for the induced streaming:

$$\tilde{\psi} = \left(\frac{\alpha\epsilon}{|C|}\right)^{\frac{1}{2}}\psi, \quad \tilde{\eta} = (\alpha\epsilon|C|)^{\frac{1}{2}}\eta. \tag{6.1}$$

The definitions of $\tilde{\xi}$ and t remain unchanged. The exact vorticity equation (5.2) is then transformed to

$$\left(\frac{\partial}{\partial t} - \alpha\cos t\frac{\partial}{\partial\tilde{\xi}}\right)\tilde{\nabla}^2\tilde{\psi} - \alpha|C|\frac{\partial\left(\tilde{\psi}, \frac{1}{J}\tilde{\nabla}^2\tilde{\psi}\right)}{\partial(\tilde{\xi}, \tilde{\eta})} = \epsilon\alpha|C|\tilde{\nabla}^2\left(\frac{1}{J}\tilde{\nabla}^2\tilde{\psi}\right), \tag{6.2}$$

where

$$\tilde{\nabla}^2 = \frac{\partial^2}{\partial\tilde{\eta}^2} + \frac{1}{R_s}\frac{\partial^2}{\partial\tilde{\xi}^2}, \tag{6.3}$$

$$J = 1 - 2\epsilon\cos(\tilde{\xi} + \alpha\sin t)\exp\left(-\frac{\tilde{\eta}}{R_s^{\frac{1}{2}}}\right) + \epsilon^2\exp\left(-\frac{2\tilde{\eta}}{R_s^{\frac{1}{2}}}\right), \tag{6.4}$$

and

$$R_s = \frac{\alpha\epsilon|C|}{\sigma^2} = \frac{Aa|C|}{\delta^2} \geqslant O(1) \tag{6.5}$$

is a Reynolds number associated with the induced streaming. Again the boundary conditions at $\tilde{\eta} = 0$ are determined so that the stream function and the tangential velocity are matched with the Stokes layer at each order.

We now introduce the expansions

$$\tilde{\psi} = \frac{\tilde{\eta}}{|C|}\cos t + \left(\frac{\alpha\epsilon}{|C|}\right)^{\frac{1}{2}}\left(\frac{e^{it}}{2\gamma} + *\right) + \epsilon\tilde{\psi}_1 + \epsilon^{\frac{3}{2}}\tilde{\psi}_{\frac{3}{2}} + \epsilon^2\tilde{\psi}_2 + \ldots \tag{6.6}$$

and

$$\frac{1}{J} = 1 + 2\epsilon\cos(\tilde{\xi} + \alpha\sin t)\exp\left(-\frac{\tilde{\eta}}{R_s^{\frac{1}{2}}}\right) + O(\epsilon^2), \tag{6.7}$$

where the first and the second terms of (6.6) are matched with the right-hand side of (5.7). The term $O(\epsilon^{\frac{3}{2}})$ is in principle needed to match with the Stokes layer. Upon substituting (6.6) and (6.7) into (6.2) we find again that $\tilde{\psi}_1$ satisfies

$$\frac{\partial}{\partial t}\tilde{\nabla}^2\tilde{\psi}_1 = 0 \tag{6.8}$$

at $O(\epsilon)$. The Stokes-layer solution which should be matched at this order is just the first term of (5.28). Thus $\tilde{\psi}_1$ can only depend on $\tilde{\xi}$ and $\tilde{\eta}$ and satisfies (6.8) trivially. At the next order, $O(\epsilon^{\frac{3}{2}})$, $\tilde{\psi}_{\frac{3}{2}}$ satisfies the same equation (6.8), and is matched with the second term of (5.28) expressed in terms of the outer stream function defined in (6.1). But it will not be needed in the sequel. At $O(\epsilon^2)$ the perturbation equation is

$$\frac{\partial}{\partial t}\tilde{\nabla}^2\tilde{\psi}_2 + \alpha\cos t\frac{\partial}{\partial\tilde{\xi}}\left\{2\cos(\tilde{\xi}+\alpha\sin t)\exp\left(-\frac{\tilde{\eta}}{R_s^{\frac{1}{2}}}\right)\tilde{\nabla}^2\tilde{\psi}_1\right\} - \alpha|C|\frac{\partial(\tilde{\psi}_1, \tilde{\nabla}^2\tilde{\psi}_1)}{\partial(\tilde{\xi},\tilde{\eta})} = \alpha|C|\tilde{\nabla}^2\tilde{\nabla}^2\tilde{\psi}_1. \tag{6.9}$$

Since
$$\cos t\cos(\tilde{\xi}+\alpha\sin t) = \frac{1}{\alpha}\frac{\partial}{\partial t}\sin(\tilde{\xi}+\alpha\sin t) \tag{6.10}$$

the time average of (6.9) gives

$$-\frac{\partial(\tilde{\psi}_1, \tilde{\nabla}^2\tilde{\psi}_1)}{\partial(\tilde{\xi},\tilde{\eta})} = \tilde{\nabla}^2\tilde{\nabla}^2\tilde{\psi}_1 \tag{6.11}$$

which is once more the steady Navier–Stokes equations. The boundary conditions at $\tilde{\eta} = 0$ follow from the first term in (5.28) (or (5.29)),

$$\tilde{\psi}_1 = 0, \quad \frac{\partial\tilde{\psi}_1}{\partial\tilde{\eta}} = (\operatorname{sgn} C)\sin\tilde{\xi}, \quad \tilde{\eta} = 0 \tag{6.12}$$

and at infinity we impose

$$\frac{\partial\tilde{\psi}_1}{\partial\tilde{\xi}} = \frac{\partial\tilde{\psi}_1}{\partial\tilde{\eta}} = 0, \quad \tilde{\eta}\sim\infty. \tag{6.13a, b}$$

Thus in the moving frame, flow in the outer layer is driven by a non-uniform tangential velocity at the lower boundary. The governing parameters of this problem are the Reynolds number R_s and the sign of the induced streaming at the outer edge of the Stokes layer. Because of the form of the boundary condition (6.12), it is only necessary to examine $C > 0$. The results can be used for negative C by shifting the origin of $\tilde{\xi}$ by π.

6.2. *Results and discussion*

The numerical solution can be carried out by the Fourier method as in §4. We show in figure 7 the induced streaming in the moving coordinates $(\tilde{\xi},\tilde{\eta})$. Within the horizontal extent of one ripple wavelength, there are two counter-rotating cells. As either α or ϵ increases, or σ decreases, the Reynolds number R_s increases; a jet is formed along $\tilde{\xi} = \pi$. The jet width decreases with R_s. In the stationary frame, the vortices and the jets, whose dimensions can be comparable with the ripple wavelength, traverse to and fro horizontally above the ripples. The amplitude of travel is equal to that of the ambient fluid and can be comparable with a ripple wavelength. This feature is consistent with the numerical results of Shum (1988) who solved the transient Navier–Stokes equations from rest. It should be mentioned that to a stationary observer the vortices can be seen only near the instant when the

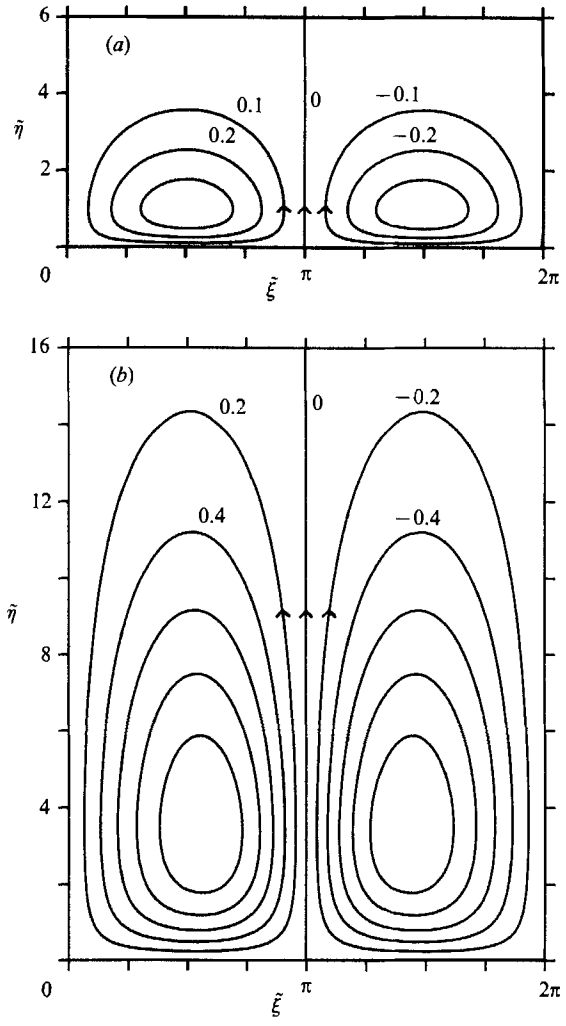

FIGURE 7(*a*,*b*). For caption see facing page.

ambient velocity vanishes. Otherwise they are overwhelmed by the $O(1)$ ambient flow.

The jet can be viewed in another manner by plotting the stream function $\tilde{\psi}_1$ at some height $\tilde{\eta}$, as shown in figure 8. Clearly the width of the upward flow becomes narrower with increasing R_s. In the limit of $R_s \sim \infty$, the $\tilde{\xi}$-derivative in the Laplacian $\tilde{\nabla}^2$ is again negligible. Equation (6.11) is integrated once to yield

$$-\frac{\partial\tilde{\psi}_1}{\partial\tilde{\xi}}\frac{\partial^2\tilde{\psi}_1}{\partial\tilde{\eta}^2}+\frac{\partial\tilde{\psi}_1}{\partial\tilde{\eta}}\frac{\partial^2\tilde{\psi}_1}{\partial\tilde{\eta}\,\partial\tilde{\xi}}=\frac{\partial^3\tilde{\psi}_1}{\partial\tilde{\eta}^3}. \tag{6.14}$$

This Blasius equation, together with boundary conditions (6.12) and (6.13*b*), can be solved numerically (see Davidson & Riley 1972). In figure 8 we also plot the result of this limiting case; the width of the jet is now infinitesimal. Our solutions are seen to converge to this Blasius solution as R_s increases.

So far we have used the $(\tilde{\xi},\tilde{\eta})$-coordinates in which vertical and horizontal lengths

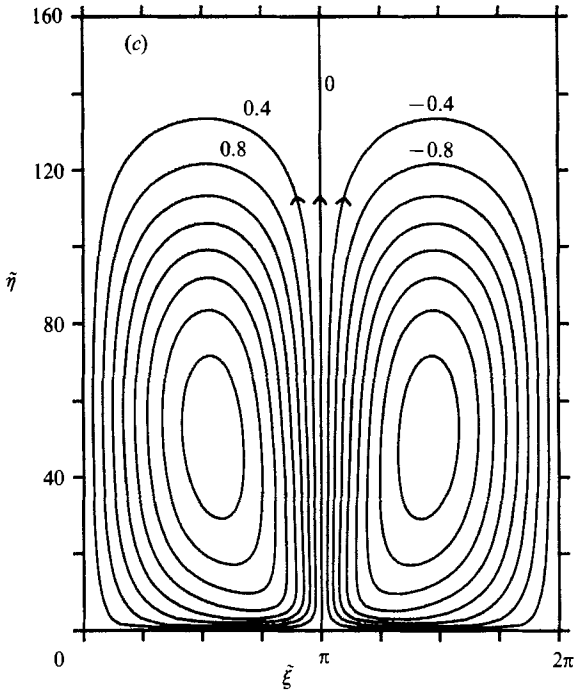

FIGURE 7. Stream-function contours of induced streaming in moving coordinates in a Stuart layer. Numbers adjacent to the streamlines represent the values of $\tilde{\psi}_1$. (*a*) $R_s = 1$, $\Delta\tilde{\psi}_1 = 0.1$; (*b*) $R_s = 10$, $\Delta\tilde{\psi}_1 = 0.2$; (*c*) $R_s = 100$, $\Delta\tilde{\psi}_1 = 0.4$, the vertical scale is reduced.

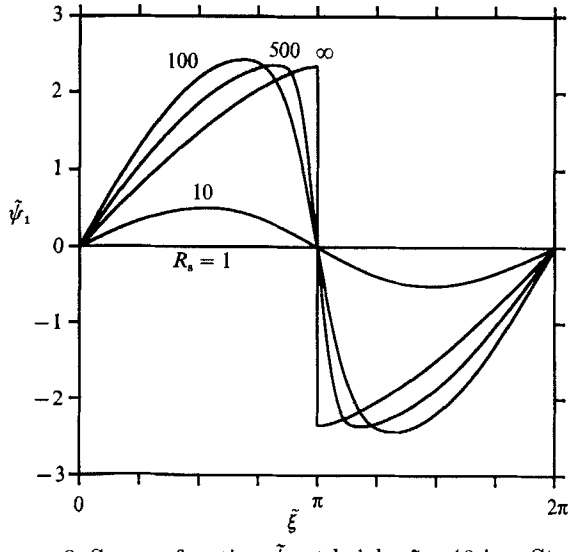

FIGURE 8. Stream function $\tilde{\psi}_1$ at height $\tilde{\eta} = 10$ in a Stuart layer.

are scaled differently. We now exhibit the vertical velocity $V = -R_s^{-\frac{1}{2}}\partial\tilde{\psi}_1/\partial\tilde{\xi}$ along the axis ($\tilde{\xi} = \pi$) as a function of undistorted vertical coordinate $k\eta'$, in figure 9, where the magnitude of the vertical velocity is normalized by the maximum induced streaming at $\tilde{\eta} = 0$. The vertical extent of the jet is seen to increase monotonically with R_s, whereas its magnitude is bounded for large Reynolds number.

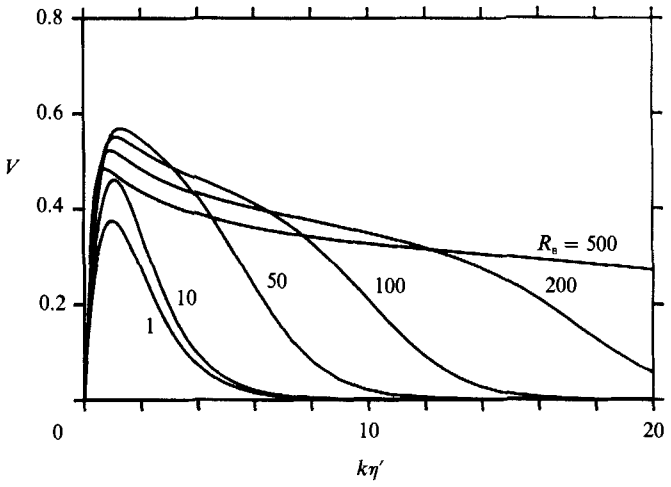

FIGURE 9. Vertical velocity along the axis ($\tilde{\xi} = \pi$) in a Stuart layer, normalized by the maximum induced streaming at $\tilde{\eta} = 0$.

The steady streaming in the stationary frame of reference is obtained as follows:

$$\tilde{\psi}_1 = \sum_1^\infty b_n(\tilde{\eta}) \sin[n(\xi - \alpha \sin t)]$$

$$= \sum_1^\infty b_n \frac{1}{2i} \sum_{-\infty}^{\infty} e^{-imt} J_m(n\alpha)[e^{in\xi} - (-)^m e^{-in\xi})]. \tag{6.15}$$

The time average is simply

$$\langle \tilde{\psi}_1 \rangle = \sum_1^\infty b_n(\tilde{\eta}) J_0(n\alpha) \sin n\xi, \tag{6.16}$$

where b_n is the Fourier coefficient defined as in (4.26). We show in figure 10 the steady streaming in the stationary frame for $\alpha = 1.1$ when $C > 0$ and CJ_0 is a positive maximum. There are two counter-rotating vortices with fluid sinking toward the crest and rising above the trough. As R_s increases from 10 to 100, the intensity of the vortices as well as their vertical extent increases. The strong upward jet now disappears owing to the time averaging in the stationary frame. For $\alpha = 4$, $C < 0$ but CJ_0 is still a positive maximum; the directions of the steady vortices remain the same. We have also computed the cases for $\alpha = 2.7$ and 5.3 when CJ_0 are negative maximum; fluid sinks toward the trough and rises above the crest. But the circulation is very weak and is not presented here.

We now comment on the works by Lyne (1971) and Vittori (1989), both of whom considered only the steady Eulerian streaming in the viscous region, where the convective inertia is never dominant. According to our argument in §1, their assumption of weak convective inertia is justified only if $R = \epsilon\alpha/\sigma^2 \ll 1$. In contrast our theory is for the more practical case of $R = \epsilon\alpha/\sigma^2 \geqslant O(1)$ where the viscous region is divided into two layers. The convective inertia is of the first-order importance in the outer layer but not in the Stokes layer. More specifically, Lyne (1971) has considered the case of $\alpha \gg 1$, $\sigma\alpha^{\frac{1}{3}} = O(1)$, and $\epsilon/\sigma \ll 1$, to the first order in ϵ/σ. He obtained steady circulations of a multi-deck pattern in the Stokes layer. This pattern is not found in our analysis even for $\alpha = 6$. Vittori, on the other hand, assumed $\alpha =$

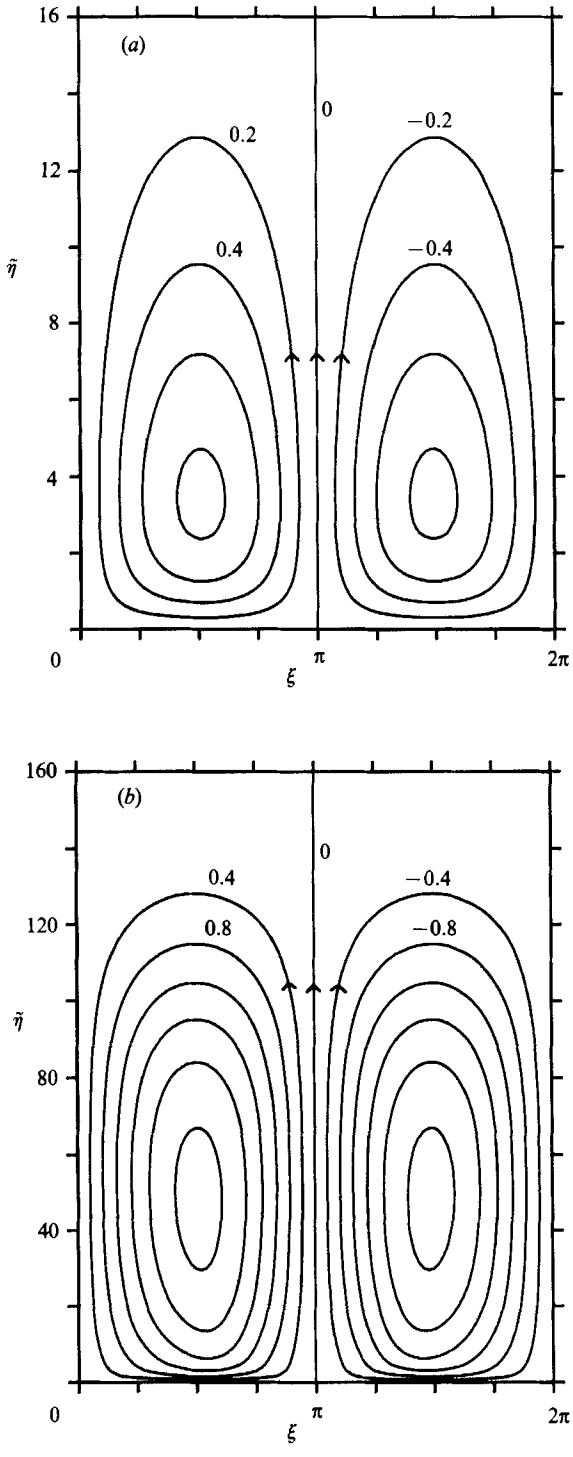

FIGURE 10. Stream-function contours of Eulerian streaming in a stationary frame of reference in a Stuart Layer. Numbers adjacent to the streamlines represent the values of $\tilde{\psi}_1$. $\alpha = 1.1$. (*a*) $R_s = 10$, $\Delta\tilde{\psi}_1 = 0.2$; (*b*) $R_s = 100$, $\Delta\tilde{\psi}_1 = 0.4$.

$O(1)$ and $a/\delta = \epsilon/\sigma \ll 1$ so that the ripples must also be completely immersed in the Stokes layer. For relatively small $\sigma(< 0.2)$, her calculations of the steady streaming in the viscous region gives four cells if $\alpha < 2.4$, but two cells if $\alpha > 2.4$. This is consistent with our results in §5, where we considered the Stokes layer and the lower edge of the outer layer, with the assumption that $\alpha = O(1)$, $\epsilon \ll 1$, and $\sigma \ll 1$ but arbitrary ϵ/σ (Only in §6 is the assumption $\epsilon/\sigma^2 \geqslant O(1)$ added). The agreement should therefore be expected. However, we have further shown that the four-cell pattern reappears for $2.95 < \alpha < 5.0$ and $\alpha > 5.5$. Outside the Stokes layer the circulation by Vittori is weak, owing to the assumption of $R \ll 1$. This is not the case in our theory, where not only is the steady streaming stronger, but the oscillating vortices are the strongest physical features, not discussed by her. For clarity, the parametric regimes of validity of the theories discussed above are also summarized in table 1.

7. Concluding remarks

While there have been theories in the past on laminar oscillatory flows over rigid ripples, we have added new analyses for the cases in which either the ripple slope or the Keulegan–Carpenter number is finite, and furthermore the Stokes boundary layer is so thin that the Reynolds number is large. The analyses are carried out under the assumption that the flow is strictly periodic in time. In the case of finite Keulegan–Carpenter number we have found that Stuart's theory, which was originally devised for time-averaged circulations, can be applied to predict vortices that are convected to and fro by an oscillatory flow. These oscillating vortices owe their existence to viscous shear in the Stokes layer below, but rise far above into the region where the latter is of no direct influence. Because of the choice of the regime of parameters, our results can in principle be simulated and tested experimentally in ordinary water.

In an earlier theory, Longuet-Higgins (1981) also treated the vortex generation by sharp-crested ripples under waves by a potential theory. In his model, discrete vortices which emanate from the sharp crests at small intervals of time, interact with one another according to the laws of potential flow. As the number of discrete vortices becomes large, their interaction becomes very complex. Longuet-Higgins then introduced a criterion to replace, at finite time intervals, the vortex clouds by a pair of point vortices, which then drift away to great heights. This physical picture is vastly different from ours. Controlled experiments are therefore needed to ascertain the realms of validity of both theories.

A major assumption made here is that the flow is periodic in time. In a nonlinear problem such as this this assumption may be realized only by a special initial condition. Recent numerical experiments (Shum 1988) by solving Navier–Stokes equations show evidence that if the periodic motion of the ambient fluid starts from rest, the response near the ripples quickly reaches a periodic state only if the Reynolds number is sufficiently small. Otherwise periodicity is not attained even after many periods permitted by the computation. The flow in the first half of a period can also be different from that in the second half. Effort and expense of such computations are however immense, and further analytical work, perhaps by examining the instability of strictly periodic solutions such as those discussed herein, may shed light on the possible transition to aperiodicity, or chaos.

We thank the US Office of Naval Research (Contract N00014-83K 0550) and

National Science Foundation (Grant MSME 8813121) for supporting this research. Part of the writing was done while C.C.M. was a visiting professor at l'Institut de Mécanique de Grenoble.

REFERENCES

BENJAMIN, T. B. 1959 Shearing flow over a wavy boundary. *J. Fluid Mech.* **6**, 161–205.

CAPONI, E. A., FORNBERG, B., KNIGHT, D. D., MCLEAN, J. W., SAFFMAN, P. G. & YUEN, H. C. 1982 Calculation of laminar viscous flow over a moving wavy surface. *J. Fluid Mech.* **124**, 347–362.

DAVIDSON, B. J. & RILEY, N. 1972 Jets induced by oscillatory motion. *J. Fluid Mech.* **53**, 287–303.

DORE, B. D. 1976 Double boundary layers in standing surface waves. *Pure Appl. Geophys.* **114**, 629–637.

HADDON, E. W. & RILEY, N. 1983 A note on the mean circulation in standing waves. *Wave Motion* **5**, 43–48.

HALL, P. 1984 On the stability of the unsteady boundary layer on a cylinder oscillating transversely in a viscous fluid. *J. Fluid Mech.* **146**, 347–367.

KANEKO, A. & HONJI, H. 1979 Double structures of steady streaming in the oscillatory viscous flow over a wavy wall. *J. Fluid Mech.* **93**, 727–736.

LIU, A.-K. & DAVIS, S. H. 1977 Viscous attenuation of mean drift in water waves. *J. Fluid Mech.* **81**, 63–84.

LONGUET-HIGGINS, M. S. 1981 Oscillating flow over steep sand ripples. *J. Fluid Mech.* **107**, 1–35.

LYNE, W. H. 1971 Unsteady viscous flow over a wavy wall. *J. Fluid Mech.* **50**, 33–48.

MATSUNAGA, N., KANEKO, A. & HONJI, H. 1981 A numerical study of steady streamings in oscillatory flow over a wavy wall. *J. Hydraul. Res.* **19**, 29–42.

MEI, C. C., LIU, P. L-F. & CARTER, T. G. 1972 Mass transport in water waves. *Ralph M. Parsons Laboratory for Water Resources and Hydrodynamics, Massachusetts Institute of Technology, Rep.* 146, 287 pp.

RALPH, M. E. 1986 Oscillatory flows in wavy-walled tubes. *J. Fluid Mech.* **168**, 515–540.

RILEY, N. 1965 Oscillating viscous flows. *Mathematika* **12**, 161–175.

RILEY, N. 1967 Oscillating viscous flows: review and extension. *J. Inst. Maths Applics* **3**, 419–434.

RILEY, N. 1984 Progressive surface waves on a liquid of non-uniform depth. *Wave Motion* **6**, 15–22.

SATO, S., MIMURA, N. & WATANABE A. 1984 Oscillatory boundary layer flow over rippled beds. In *Proc. 19th Conf. on Coastal Engng.* pp. 2293–2309.

SCHLICHTING, H. 1955 *Boundary-Layer Theory.* McGraw-Hill.

SHUM, K. T. 1988 A numerical study of vortex dynamics over rigid ripples. Ph.D. Thesis, M.I.T.

SLEATH, J. F. A. 1974*a* Mass transport over a rough bed. *J. Mar. Res.* **32**, 13–24.

SLEATH, J. F. A. 1974*b* Stability of laminar flow at seabed. *J. Waterways Harbors and Coastal Engng Div. Proc. ASCE* **100** (WW2), 105–122.

SLEATH, J. F. A. 1975 A contribution to the study of vortex ripples. *J. Hydraul. Res.* **13**, 315–328.

SOBEY, I. J. 1980 On flow through furrowed channels. Part 1. Calculated flow patterns. *J. Fluid Mech.* **96**, 1–26.

SOBEY, I. J. 1982 Oscillatory flows at intermediate Strouhal number in asymmetric channels. *J. Fluid Mech.* **125**, 359–373.

SOBEY, I. J. 1983 The occurrence of separation in oscillatory flow. *J. Fluid Mech.* **134**, 247–257.

STUART, J. T. 1963 Unsteady boundary layers. In *Laminar Boundary Layers*, pp. 349–408. Oxford University Press.

STUART, J. T. 1966 Double boundary layers in oscillatory viscous flow. *J. Fluid Mech.* **24**, 673–687.

VITTORI, G. 1989 Non-linear viscous oscillatory flow over a small amplitude wavy wall. *J. Hydraul. Res.* **27**, 267–280.

WANG, C. Y. 1968 On high-frequency oscillatory viscous flows. *J. Fluid Mech.* **32**. 55–68.